Ad Hoc Networks 111 (2021) 102342

Contents lists available at ScienceDirect

Ad Hoc Networks

journal homepage: www.elsevier.com/locate/adhoc

Energy balancing in mobile opportunistic networks with wireless charging: Single and multi-hop approaches

Aashish Dhungana, Eyuphan Bulut *

Department of Computer Science, Virginia Commonwealth University, 401 West Main St. Richmond, VA 23284, USA

ARTICLE INFO

Keywords:
Energy balancing
Wireless energy transfer
Mobile opportunistic network
Network lifetime

ABSTRACT

Leveraging peer-to-peer energy sharing solutions between nodes, energy balancing aims to balance energy among the nodes in a network towards prolonging the network lifetime especially when external energy supply is not available. Previous studies target an energy balance among the devices as fast as possible but they waste energy in the network during this process due to the excessive interactions between nodes. Moreover, they do not take into account different contact relations between the nodes in the network. In this paper, we address these issues and present efficient and loss-aware energy balancing protocols considering the contact graph heterogeneity between nodes and a time threshold for completing the energy balancing. We consider both the single hop and multi-hop based energy exchanges among nodes and design separate protocols for each. Through simulations, we show that the proposed algorithms outperform the state-of-the-art solution by reaching a better energy balance with a lower energy loss, and multi-hop based approach performs better than single hop based one. We also discuss the implications of energy balancing process on network lifetime through different use cases and provide the necessary modifications on the proposed system to maximize the network lifetime especially in disconnected networks.

1. Introduction

Energy is a vital but scarce resource in mobile networks comprised of battery-powered devices. It affects the success of collaborative network operations (e.g., multi-hop routing) as well as the network lifetime. Many studies have been performed to develop efficient energy management strategies in mobile networks leveraging different methods (e.g., sleep scheduling [1], harvesting [2], cross-layer design [3]). With the recent advances in wireless power transfer (WPT) technology, wireless charging based energy replenishment of mobile nodes has also been considered as an alternative solution for continuous operation of such networks. There are many studies performed especially for wireless sensor networks [4–6] that use mobile chargers, which are special vehicles (e.g., robot, Unmanned Aerial Vehicle (UAV)) with high energy supplies, to charge the sensors in the field periodically. Recently, wireless charging of different types of mobile devices/vehicles such as smartphones [7–9], electric vehicles [10–12] and Internet-of-Things (IoT) devices [13–15] has also been considered.

While most of the aforementioned studies consider the charging of mobile nodes (e.g., devices or vehicles) wirelessly from a mobile charger node or from a direct energy source, it may not be practical to utilize an external charger in some networking scenarios due to environmental restrictions and operational costs. In such cases, leveraging the available resources among nodes in the network could help. For example, in the context of mobile social networks, friends can help charge each other to charge their devices (i.e., crowdcharging [9,16,17]) utilizing the bidirectional energy sharing capability of recent smartphones (e.g., Samsung Galaxy S10, Huawei Mate 20 Pro). This could be motivated by reciprocal altruism among friends [18] or through incentives [19]. Note that the current form of wireless charging (e.g., inductive charging standard Qi [20]) integrated in most of the products in the market today requires very close distances (i.e., almost touching) for energy transfer, however it is still a more convenient method than energy sharing over cables [21] or charging the devices from outlets. Such a peer-to-peer energy sharing can also be critical during disasters or emergency situations when the energy is scarce. For example, several members of a family or close friends can share the total available energy in their phone batteries equally to stay connected longer during searching of another member of the team separately. Moreover, the charging of IoT devices could also be realized through crowdsourcing of energy from the smart mobile devices of people [15,19,22,23].

In this paper, we study the energy balancing problem that leverages the bidirectional energy sharing capabilities of nodes [9,16,17] and aims to efficiently use the available energy at nodes to prolong the

* Corresponding author.
E-mail addresses: dhunganaa@vcu.edu (A. Dhungana), ebulut@vcu.edu (E. Bulut).

https://doi.org/10.1016/j.adhoc.2020.102342
Received 17 June 2020; Received in revised form 12 October 2020; Accepted 13 October 2020
Available online 22 October 2020

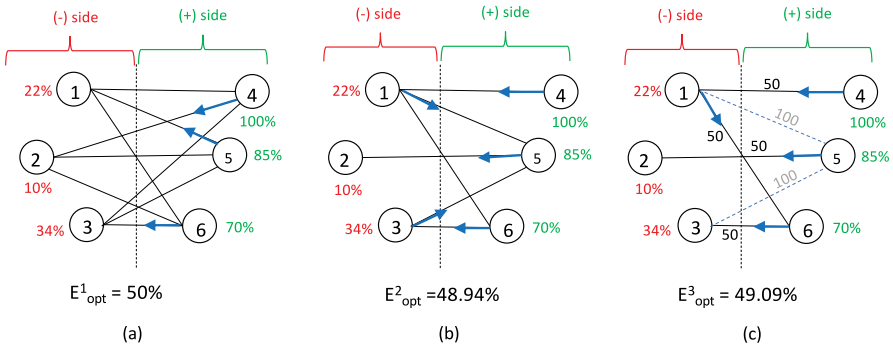

Fig. 1. Energy balancing scenarios: (a) With a fully connected contact graph, (b) With a partially connected contact graph, (c) With time limit of 50. Edges represent that the nodes meet each other opportunistically with an average intermeeting time shown as edge weight.

Table 1
Energy transfer amounts between nodes and final energy levels of nodes for scenarios in Fig. 1 with 80% transfer efficiency.

Scenario	Energy transfer amounts	Final energy levels of nodes					
		1	2	3	4	5	6
Fig. 1a	④ $\xrightarrow{50\%}$ ②, ⑤ $\xrightarrow{35\%}$ ①, ⑥ $\xrightarrow{20\%}$ ③	50% for all nodes					
Fig. 1b	⑤ $\xrightarrow{48.68\%}$ ②, ⑥ $\xrightarrow{21.05\%}$ ③, ④ $\xrightarrow{51.05\%}$ ①, ① $\xrightarrow{13.89\%}$ ⑤, ③ $\xrightarrow{1.89\%}$ ⑤	48.94% for all nodes					
Fig. 1c	⑤ $\xrightarrow{35.90\%}$ ②, ⑥ $\xrightarrow{31.81\%}$ ③, ④ $\xrightarrow{50.90\%}$ ①, ① $\xrightarrow{13.63\%}$ ⑥	49.09%	38.72%	59.45%		49.09%	

network lifetime, which is usually defined as the time until the first node in the network dies. Energy balancing is the process of equalizing the energy levels at each node or minimizing the sum of the differences of their energy from the average energy (i.e., variation distance as will be detailed later) in the network as much as possible. In opportunistic networks, energy balancing is achieved through energy exchanges between nodes as they meet. However, in every energy exchange there will be an energy loss due to the imperfect efficiency in the current wireless charging technologies. Thus, the challenge is to achieve an energy balance among nodes while also minimizing the energy loss during this process.

The current solutions [24–27] for energy balancing assume that all the nodes in the network meet with each other with an equal probability. However, in opportunistic networks [28,29], each node may only meet with a subset of nodes in the network, thus there may not be an opportunity for energy exchange between some pairs of nodes directly. Moreover, for some node pairs that meet, the average intermeeting times can be very large, thus the energy exchanges can only occur rarely, resulting in a very long time until an energy balance in the network is achieved.

1.1. Motivating example

We illustrate the effects of these limitations in the energy balancing process through an example with 6 nodes as shown in Fig. 1. We consider three different scenarios in which energy levels of nodes are the same but the contact graphs between nodes are different. If each node on the negative side (i.e., having energy less than the average energy in the network (53.5%)) has an opportunity to meet with each node on the positive side as in Fig. 1a, the energy sharing process will be relatively easy. For example, with an 80% transfer efficiency (or with an energy loss rate of 0.2), the optimal average energy reachable by all nodes will be 50%, which happens when node 5 transfers 35% to node 1 (which only gets 28% due to loss), node 4 transfers 50% to node 2 (which only gets 40%) and node 6 transfers 20% to node 3 (which only gets 16%).

On the other hand, when there is no direct energy exchange opportunity between some negative and positive side node pairs, as in the case of Fig. 1b, the optimal energy achievable can be less due to the more number of interactions required between nodes and multi-hop travel of energy, causing additional loss. In Fig. 1b, nodes still reach a perfect energy balance (i.e., all nodes having the same energy level) at 48.94% through transfer amounts shown in Table 1, however, the final balanced energy level is less than it is in Fig. 1a (which has a complete contact graph between all positive and negative side nodes). Finally, there can be a time threshold for reaching an energy balance. In that case, we can simply ignore the edges (i.e., contact relations) with an average intermeeting time higher than this threshold and recalculate the average optimal energy balance. Fig. 1c shows the situation where the deadline for energy balance is set to 50 time units. The dotted edges shown in the figure are ignored; hence, nodes cannot use these edges for energy exchanges. In this case, the optimal average energy balance is 49.09%, however, as it is shown in Table 1, not all nodes can reach this energy level. This example shows that with sparse contact graphs, the optimal energy balance can change and not all nodes may reach that.

1.2. Contributions

In this paper, we address these challenges in achieving an energy balance among the nodes in a mobile opportunistic network. Within the given contact graph limitations, average intermeeting times for the meeting pairs, and the time threshold to complete balancing, we aim to first minimize the energy difference between nodes and then minimize the energy loss during this process. To this end, we utilize Mixed Integer Linear Programming (MILP) to find out the optimal energy balance possible with a minimal energy loss and develop corresponding energy sharing protocols among nodes considering single hop and multi-hop energy exchanges separately. Finally, we also discuss how the energy balancing problem translates to the problem of network lifetime maximization and provide the necessary updates in the optimization model in disconnected networks. Through simulations, we show that

our algorithms overcome the state-of-the-art solution by achieving a higher energy balance with a lower energy loss and a longer network lifetime. We also show the benefit of multi-hop based solution over single hop solution in sparse networks. The main contributions of this paper can be summarized as follows:

- We find out the optimal energy balance possible for a given contact graph of nodes and intermeeting times through direct energy exchanges (i.e., single hop) using MILP.
- We develop two different energy balancing protocols among nodes based on the required energy exchanges found by MILP model to reach the optimal energy balance.
- For networks with sparse contact graphs, we enhance the MILP model to allow multi-hop energy exchanges to achieve a better energy balance and develop the corresponding energy balancing protocol among nodes considering both the direct and relayed energy exchanges.
- We discuss the relation of the energy balancing problem to the problem of network lifetime maximization and provide the updates needed in the MILP model in disconnected graphs.
- We perform extensive simulations using meeting patterns from synthetic and real user traces and show that the proposed energy sharing protocols perform better than the state-of-the-art.

The preliminary version of this study is published in [30] considering only the single hop based energy exchanges. In this paper, we also consider the multi-hop based energy exchanges and develop corresponding MILP based optimization model as well as the energy sharing protocol. The relation between the energy balancing and network lifetime maximization problems is also discussed in this version and new simulation results are provided regarding the extended content.

The rest of the paper is structured as follows. In Section 2, we discuss the related work. In Section 3, we provide the system model, our assumptions and the problem statement. In Section 4, we elaborate on the MILP based solution with single hop energy exchanges and the energy sharing protocols among nodes in the network. In Section 5, we extend the MILP based solution by using multi-hop based energy exchanges and develop the corresponding energy sharing protocol among nodes. In Section 6, we present the simulation settings and results comparing the performance of the proposed algorithms with the state-of-the-art solution. In Section 7, we discuss the implications of energy balancing in terms of network lifetime and provide the necessary modifications in MILP model and solutions in case of disconnected networks. Finally, we conclude the paper and outline the future work in Section 8.

2. Related work

2.1. Mobile opportunistic networks

Mobile opportunistic networks are mobile ad hoc and infrastructureless networks that are most of the time disconnected and thus exploit node mobility to opportunistically interact (e.g., share data or energy) with each other. The communication between nodes usually happens in direct manner through wireless network interfaces of the devices (e.g., Wi-Fi, Bluetooth). Multi-hop communication is also made possible utilizing store-carry-and-forward paradigm. Examples of such opportunistic networks include mobile social networks [31] and vehicular opportunistic networks [32], where mobility of devices are defined by people and vehicles, respectively. In the literature, most of the initial studies have focused on the routing problem [33], but various other problems such as mobility modeling [29], opportunistic computing [34], security, trust [35] and privacy [36] management, and realistic simulation [28] have also been studied.

Thanks to the recent advances in wireless power transfer (WPT) technology and its adoption in various mobile devices, problems leveraging energy sharing between nodes have also been considered in the domain of mobile opportunistic networks to optimize several network operations. There are various WPT technologies (e.g., inductive charging, magnetic resonant coupling, and RF charging) with different advantages and disadvantages [37]. Initial studies leveraging wireless charging or WPT have focused on sensor networks and considered charging scheduling of mobile charger vehicles (MCV) which recharge these sensors periodically. We refer the interested readers to [37,38] for overview of wireless charging technologies and its applications in sensor networks in general. Note that these studies most of the time exploit one-way energy transfer between network nodes (i.e., chargers to sensors). Bi-directional wireless energy transfer has recently been considered in mobile opportunistic networks which are discussed in next section.

2.2. Energy sharing in mobile opportunistic networks

In this part, we specifically overview the studies that utilize wireless charging in mobile opportunistic networks, in particular through peer-to-peer energy sharing among peers. Peer-to-peer energy sharing [17] has been utilized to achieve several different goals in a mobile opportunistic network. It has been considered among mobile chargers [5] to build a collaborative and energy efficient charging scheduling, for crowd charging of devices (i.e., smartphones) by other devices [39–43] and to promote opportunistic content delivery by providing energy as an incentive [44–46] to the devices to carry the message for others.

There are also several studies [24–26] that utilize peer-to-peer wireless energy exchange to balance the energy within a mobile opportunistic network and propose various energy sharing protocols. In some other studies, this process has also been modeled by taking into account the network structure and formation [47,48] as well as online social network relations [18] among users. While these works can decrease the variation distance between the energy levels of nodes and the average energy in the network quickly, they do suffer from high energy loss in the network by design. This is because they let the nodes in the opposite sides of the current average energy level in the network interact and exchange energy at every opportunity, causing the nodes change their side with respect to average energy several times and lose energy unnecessarily. This has been partially addressed in [27] but it is assumed that all nodes in the network has an opportunity to interact (i.e., meeting) with each other, which may not be the case for opportunistic networks. Thus, in this paper, we address the energy balancing problem considering the incomplete contact graphs among nodes as well as a time threshold to achieve the balancing. We model and study the optimization problem when both the single hop and multi-hop interactions are allowed for energy exchanges between nodes. Through simulations we show that the proposed algorithms show better performance than the state-of-the-art thanks to their designs that aim an energy exchange only in useful interactions between nodes. Moreover, we show that multi-hop energy exchanges can help decrease the variation distance in energy distribution further especially in sparse networks.

In Table 2, we provide a summary and comparison of existing works and show how our study differs from them. Here, we divide the existing literature on energy sharing into three categories based on their objectives, namely, Crowd Charging (CD), Content Delivery (CD) and Energy Balancing (EB). Our study fits to the EB category and it provides enhancements to the existing work by several means. First, we provide energy balancing solutions for different and incomplete contact graphs as opposed to the existing work which requires the network to be fully connected. Second, we analyze how the existing protocols cause unnecessary energy loss in the network and provide solutions to overcome this problem by integrating the final reachable energy balance in the balancing decision process. Third, we benefit from both single-hop and multi-hop (if needed) energy sharing among nodes to reach out the perfect balance, if possible.

Table 2
Summary of research utilizing energy sharing in mobile opportunistic networks (**CC**: Crowd Charging, **CD**: Content Delivery, **EB**: Energy Balancing).

	Objective			Key drawback	Sharing characteristic		
Ref	CC	CD	EB		Direction	Hop	Deadline
[5]	✓			Only mobile chargers share energy	Limited Two-way	Single	✓
[24–26]			✓	Equal meeting probability, high energy loss	Two-way	Single	✗
[27]			✓	Full contact graph assumed	Two-way	Single	✗
[39–42]	✓			Sharing happens between certain pairs	Two-way	Single	✗
[43]	✓			Two battery units assumed at nodes	One-way	Single	✗
[44–46]		✓		Energy is used as incentive only	One-way	Single	✗
[47,48]			✓	Unnecessary energy loss	Two-way	Single	✗
[18]			✓	Relies on online social network information	Two-way	Single	✗
This study			✓		Two-way	Multiple	✓

Table 3
Notations.

Notation	Description
m	Number of nodes in the network.
$\mathcal{P}$	Interaction protocol between nodes for energy exchange.
β	Energy loss rate.
τ	Time threshold to complete energy balancing process.
p	Minimum expected meeting probability by time threshold.
$E_t(u)$	Energy of user u's device at time t.
$E_t(\mathcal{M})$	Total energy of a set $\mathcal{M}$ of nodes at time t.
$\lambda_{i,j}$	Meeting rate between nodes i and j.
$\overline{E_t}$	Average energy in the network at time t.
E_{opt}	Optimal average energy achievable in the network with minimum variation distance possible.
$\delta(P,Q)$	Total variation distance between two distributions, P, Q.
$\mathcal{E}_t(u)$	Ratio of node u's energy to the total energy in the network at time t.
$\mathcal{E}_t$	Energy distribution at time t on a sample space $\mathcal{M}$.
$\epsilon_{u,u'}$	The amount of energy exchanged from u to u'.
$\mathcal{L}$	The total energy loss in the network due to the energy exchanges.
$E_f(u)$	The final energy level of node u at the end of energy balancing process.
$\epsilon^s_{u,u'}$	The amount of u's self energy that is shared to u'.
$\epsilon^o_{u,u'}$	The amount of relayed energy from u to u' for other sources.
h_s	Total number of single hop energy exchanges used.
h_m	Total number of multi-hop energy exchanges used.
$\boldsymbol{L}_{u,u'}$	Minimum hop distance from node u to node u'.

3. System model

3.1. Assumptions

We assume a set of m nodes denoted by $\mathcal{M} = \{u_1, u_2, \dots, u_m\}$ in a mobile network. Each node is assumed to have equal battery capacity and necessary hardware for sending and receiving energy. As in previous work [18,24–27], for simplicity, we also do not consider energy loss due to mobility or other activities of the nodes.

When two nodes meet, they exchange energy according to an interaction protocol $\mathcal{P}$. The energy level of a node u at time t is denoted by $E_t(u)$, which is assumed to be between 0 and 1 (i.e., 100%). We assume each pair of nodes, (u_i, u_j), meets in an exponentially distributed manner with a rate of $\lambda_{u_iu_j}$ (i.e., average intermeeting time is $1/\lambda_{u_iu_j}$) similar to many studies (e.g., [49–52]) in mobile opportunistic networks. We also assume an energy loss rate, $\beta \in [0, 1)$, which is assumed to be a constant and depends on the technology and the equipment used. When two nodes u and u' interact at time t and node u transfers ϵ energy to node u', node u' will receive $(1-\beta)\epsilon$ energy and their new energy levels will be:

$$\begin{aligned}(E_t(u), E_t(u')) &= \mathcal{P}(E_{t-1}(u), E_{t-1}(u')) \\ &= (E_{t-1}(u) - \epsilon, E_{t-1}(u') + (1-\beta)\epsilon)\end{aligned}$$

As the interaction between u, and u' does not affect the energy levels of any other nodes, the energy levels of all other nodes remain unchanged. The notations used throughout the paper are summarized in Table 3.

3.2. Problem description

The goal is to achieve an energy balance among a population of nodes with a minimum possible variation within a given time threshold τ while minimizing the energy loss due to the energy transfers among nodes. We define the energy difference among nodes using the total variation distance from probability theory as in [18,24–27].

Let P, Q be two probability distributions defined on a sample space $\mathcal{M}$. The total variation distance is calculated as:

$$\delta(P, Q) = \sum_{x \in \mathcal{M}} |P(x) - Q(x)| \tag{1}$$

Here, we do not divide the sum by two for the sake of keeping the actual differences. In our context, the total variation distance between the current energy distribution of nodes and the target energy distribution, where all nodes have the same energy, needs to be calculated. Note that the target energy level will not be equal to the current average energy in the network, as during the energy exchanges to balance energy among nodes, there will be some energy loss. This will make the average energy level decrease over time after each interaction. At any time, we define the energy distribution $\mathcal{E}_t$ on a sample space $\mathcal{M}$ by

$$\mathcal{E}_t(u) = \frac{E_t(u)}{E_t(\mathcal{M})}, \text{where, } E_t(\mathcal{M}) = \sum_{x \in \mathcal{M}} E_t(x)$$

for any $u \in \mathcal{M}$. We also define the average energy in the network at time t

$$\overline{E_t} = \frac{E_t(\mathcal{M})}{m} \tag{2}$$

Note that in a network with a contact graph that connects all nodes (i.e., connected network), the perfect balance with zero variation distance can always be achieved. However, depending on the hop distances between nodes in the contact graph, and energy level distribution of nodes, the optimal energy level may be different. For example, for a network with a complete contact graph between nodes, as each negative side node has the opportunity to exchange energy with any positive side node as shown in Fig. 1a, it is relatively easy to compute the optimal balanced energy for all nodes [27]. Moreover, when $m \to \infty$, for a uniformly distributed energy levels of nodes, the final optimal balanced energy can be computed as [27]:

$$E_{opt} = \frac{-(1-\beta) + \sqrt{(1-\beta)}}{\beta}$$

However, in networks with incomplete contact graphs (i.e., heterogeneous relations), this will be harder to compute, thus we model it as an MILP problem and solve accordingly. On the other hand, MILP solver requires a centralized knowledge at a server or node about the energy

levels of all nodes in the network. Thus, if reaching the minimum possible variation distance is not strictly required (or sharing of energy levels is considered not practical), the decentralized protocol in our previous work [27] can always be used to achieve a variation distance as good as in previous work [24–26] but with a much smaller energy loss.

4. Energy balancing with single hop energy exchanges

In this section, we consider the case where only single hop energy exchanges are allowed between nodes. That is, each node is able to transfer energy only to its immediate neighbors and the total shareable energy is limited to its available energy. This makes the process easy as nodes can use every meeting opportunity with other nodes to share energy without waiting to receive any energy from some others. Below, we first provide a MILP based solution to find the optimal energy level for a given connected contact graph of any size and given characteristics of node relations (e.g., intermeeting time). Utilizing MILP results, we then propose two different energy balancing protocols.

4.1. Optimal energy balance

In a given mobile opportunistic network contact graph[1] and the initial energy levels of nodes, we can find the optimal energy balance achievable among nodes by MILP. Note that solving the MILP model is a one-time process which happens at the beginning. Also, it requires only one of the nodes or another centralized authority (not a node) know the energy levels of nodes, which could be achieved through cellular communication at the beginning of the process. Once the model computes the optimal balanced energy level (E_{opt}) and necessary energy exchanges between nodes to reach that level, each node is communicated with only the information of their own energy exchanges with others.

In this paper, we target an energy balance with minimum possible energy variation distance first. Then, we target minimum loss without sacrificing the variation distance. Especially, when there are multiple ways (i.e., energy exchange schedules between nodes) of reaching the same variation distance (e.g., zero), utilizing the one that will result in the minimum energy loss is important. Depending on the application requirements, it is possible to consider other objective functions with weighted combinations of variation distance and loss in a similar way.

Let $\epsilon_{u,u'}$ denote the amount of energy transferred from u to u' and $E_f(u)$ denote the final energy level of node u at the end of energy balancing process. Then,

$$E_f(u) = E_0(u) - \sum_{\forall u'} \epsilon_{u,u'} + \sum_{\forall u'} \epsilon_{u',u}(1-\beta)$$

Let also $\mathcal{L}$ denote the total energy loss in the network due to the energy exchanges between nodes during the balancing process. Then,

$$\mathcal{L} = \sum_{\forall u} \sum_{\forall u' \neq u} \epsilon_{u,u'}\beta$$

The objective is to minimize the variation distance between the final energy distribution of nodes, $\mathcal{E}_f$, and the final uniform energy distribution, $\mathcal{U}_f$, where all nodes have energy equal to the average energy in the final network (i.e., $E_f(u) = \overline{E_f}\ \forall u$) as much as possible and then minimize the total loss in the network. More formally:

$$\min \quad \delta(\mathcal{E}_f, \mathcal{U}_f)m + \mathcal{L} \tag{3}$$

$$\text{s.t.} \quad 0 \leq \epsilon_{u,u'} \leq E_t(u) l_{uu'} \qquad \forall (u,u') \tag{4}$$

$$0 \leq \sum_{\forall u' \neq u} \epsilon_{u,u'} \leq E_t(u) \qquad \forall u \tag{5}$$

$$k_{uu'} + k_{u'u} \leq 1 \qquad \forall (u,u') \tag{6}$$

$$\text{where} \quad \epsilon_{u,u'} \text{ is a decimal in } [0,1] \qquad \forall (u,u') \tag{7}$$

$$k_{uu'} = \begin{cases} 1, & \text{if } \epsilon_{u,u'} > 0 \\ 0, & \text{otherwise} \end{cases} \qquad \forall (u,u') \tag{8}$$

$$l_{uu'} = \begin{cases} 1, & \text{if } (1 - e^{-\lambda_{uu'}\tau}) \geq p \\ 0, & \text{otherwise} \end{cases} \qquad \forall (u,u') \tag{9}$$

In objective function (3), as we give priority to the minimization of variation distance over minimization of loss, we use scalarization method and multiply the former with a constant that is larger than the maximum possible value for $\mathcal{L}$. That is, we select the constant as m as each node's energy can be at most 100% or 1 and there are m nodes in the network, making the total possible loss at most $m\beta$. With a non-zero β, this guarantees that the optimization prefers a decrease in variation distance over any decrease in loss. (4) allows energy sharing between the nodes that are expected to meet within given time threshold τ as when $l_{uu'} = 0$ or no meeting is expected, no sharing will be allowed (i.e., $\epsilon_{u,u'}$ should be zero) and (5) limits the total energy sharing from each node to any other node by its available energy. This is to take into account the fact that all the energy sharing events can happen earlier than any energy receiving event potentially due to the opportunistic and non-deterministic nature of meetings between nodes. We also do not allow unnecessary two-way energy exchanges between nodes via (6). In order to determine if the nodes will meet by the time threshold, in (9), we use a predefined probability, p, and set the link between nodes to 1 if the CDF of expected meeting by time threshold is more than p.

Note that the optimal average energy level will be equal to the average energy in the final network. That is,

$$E_{opt} = \frac{\sum_{x \in \mathcal{M}} E_f(x)}{m}. \tag{10}$$

4.2. Energy balancing protocols

After the optimal energy balance and the corresponding required energy exchanges (i.e., $\epsilon_{u,u'}$) between nodes to reach that optimal balance is computed via an MILP solver, we propose two different energy balancing protocols to define the actual energy exchanges during the opportunistic meetings between pairs of nodes.

In the first protocol, we require each node to follow the exact energy exchange schedule found by the MILP solution (hence, named *L*inear *E*xact or $\mathcal{P}_{LE}$ in short). Thus, each node waits for meeting with the nodes that it is supposed to perform an energy exchange with and exchanges energy only in the amount it is allowed to do so with them. This protocol will let the nodes reach the optimal variation distance in the network eventually but due to the non-deterministic nature of opportunistic meeting patterns, it may cause nodes wait longer than expected as well as cause them miss the advantage of any earlier meeting opportunity with some unexpected nodes.

In the second protocol, we aim to benefit from the non-deterministic meetings between nodes which may let the nodes reach the target energy level earlier, thus we do not require nodes to follow the energy exchange schedule found by the MILP solution. Optimal target average energy level, E_{opt} is still found by MILP (using (10)) as in the case of first protocol, however, the nodes do not need to wait specifically for the nodes that they are supposed to exchange energy with. Instead, they make their own decisions and whenever two nodes from opposite sides of E_{opt} meet, they utilize this opportunity and update their energy towards the target. Here, in order to prevent nodes from switching their sides as in the case of previous work and causing unnecessary additional energy loss, we give priority to the node whose energy is closer to the target and let it reach that target by receiving or sharing energy with the other node. We name this protocol *O*pportunistic *C*loser or $\mathcal{P}_{OC}$ in short. Note that this protocol takes the benefit of any opportunistic meeting for energy exchange besides the scheduled ones,

[1] This can be obtained from historical meeting patterns of nodes and thanks to the long-term regularities [53–55] in node relations, it can be used for predicting future meetings.

Algorithm 1: Single Hop Energy Balancing ($\mathcal{P}$, u, u', t)

Input: (u, u'): Interacting nodes
t: Time of interaction
E_{opt}: Optimal average energy from MILP

1 $(u^+, u^-) \leftarrow (null, null)$
2 **if** $(E_{t-1}(u) > E_{opt}$ ***and*** $E_{t-1}(u') < E_{opt})$ **then**
3 $(u^+, u^-) \leftarrow (u, u')$
4 **else**
5 **if** $(E_{t-1}(u) < E_{opt}$ ***and*** $E_{t-1}(u') > E_{opt})$ **then**
6 $(u^+, u^-) \leftarrow (u', u)$
7 **if** (u^+, u^-) *is not null* **then**
8 **if** $\mathcal{P} = \mathcal{P}_{OC}$ **then**
9 $\delta_{t-1}(u^+) = E_{t-1}(u^+) - E_{opt}$
10 $\delta_{t-1}(u^-) = E_{opt} - E_{t-1}(u^-)$
11 **if** $\delta_{t-1}(u^+)(1-\beta) > \delta_{t-1}(u^-)$ **then**
12 $\mathcal{P}_{OC}(E_{t-1}(u^+), E_{t-1}(u^-)) = (E_{t-1}(u^+) - \frac{\delta_{t-1}(u^-)}{(1-\beta)}, E_{opt})$
13 **else**
14 $\mathcal{P}_{OC}(E_{t-1}(u^+), E_{t-1}(u^-)) = (E_{opt}, E_{t-1}(u^-) + (1-\beta)\delta_{t-1}(u^+))$
15 **else**
16 **if** $\epsilon_{u^+,u^-} > 0$ **then**
17 $\mathcal{P}_{LE}(E_{t-1}(u^+), E_{t-1}(u^-)) = (E_{t-1}(u^+) - \epsilon_{u^+,u^-}, E_{t-1}(u^-) + (1-\beta)\epsilon_{u^+,u^-})$
18 **else**
19 **if** $\epsilon_{u^-,u^+} > 0$ **then**
20 $\mathcal{P}_{LE}(E_{t-1}(u^+), E_{t-1}(u^-)) = (E_{t-1}(u^+) + (1-\beta)\epsilon_{u^-,u^+}, E_{t-1}(u^-) - \epsilon_{u^-,u^+})$

however, it can cause nodes not reach the optimal energy levels due to the divergence from the schedule that will make them reach the optimal energy balance. This may especially adversely affect the performance when the contact graph in the network is sparse.

We show the details of these two energy balancing protocols in Algorithm 1. For $\mathcal{P}_{OC}$ protocol (lines 8–14), if the node in the negative side, u^-, needs less than the energy that the node in the positive side, u^+, can give after loss, u^- is given priority to reach the target. The amount of energy that u^+ has to transfer should consider the loss; thus, it should be more than what u^- will actually need (lines 11–12). Otherwise, u^+ is given priority to reach the target and the energy of u^- is increased accordingly (line 14). For $\mathcal{P}_{LE}$ protocol (lines 16–20), the energy of nodes are simply updated based on the scheduled energy exchanges between nodes. Note that by MILP formulation design either ϵ_{u^+,u^-} or ϵ_{u^-,u^+} will be more than zero at the same time, however, it is possible that both could be zero as the optimal schedule may not recommend an interaction between them even though they are in opposite sides of the average energy level.

5. Energy balancing with multi-hop energy exchanges

In the previous section, we study the energy balancing problem when each node can transfer energy only to its immediate neighbors in contact graph. However, this may result in an imperfect energy balance (i.e., non-zero variation distance) especially in sparse networks. Hence, in this section, we relax this constraint and allow the nodes to exchange energy using multiple hops. Note that multi-hop transactions considered in this paper consist of consecutively performed single hop transactions at opportunistic meetings of nodes at different times. Thus, they are as practical as single hop transactions but just take longer. On the other hand, multi-hop transactions can suffer from high energy

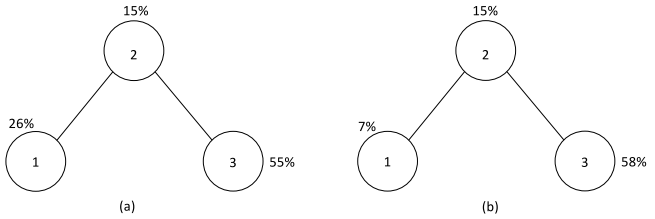

Fig. 2. An example contact graph with 3 nodes: (a) Perfect energy balancing is possible with single hop energy exchanges. (b) Perfect energy balancing requires multi-hop energy exchanges (with $\beta = 0.2$).

losses. Thus, we consider multi-hop transactions only when they help reach better energy balancing (i.e., smaller variation distance) than single hop transactions. We also design the MILP model for multi-hop case by prioritizing single-hop exchanges over multi-hop ones; thus, if both can achieve the same variation distance, single-hop transactions are utilized to minimize the loss.

Multi-hop transactions allow nodes with higher energy to give energy to nodes with low energy even though they are not meeting directly (i.e., distant in contact graph). For example, in Fig. 2a, the optimal energy achievable is 30% by all nodes (i.e., perfect energy balance with zero variation distance) with the total energy loss of 6%. This happens when node 2 gives 5% to node 1 and gets 25% from node 3, making energy levels of all nodes equal to $E_{opt} = 30\%$. Note that all energy exchanges to reach perfect balance happen between direct neighbors and the initial energy levels of nodes is more than the energy that their neighbors need to take from them (e.g., node 2 has 15% initially and just sends 5% to node 1).

However, for the example shown in Fig. 2b, this is not the case. A perfect energy balance at 23% is possible, but node 3 should share its energy with node 1 and node 2 to make that happen. Note that node 2 cannot make node 1 reach 23% by the energy it has, as it needs to transfer 20% to node 1 but it has less than that. Thus, it has to wait for receiving energy from node 3 first. This requires a multi-hop based energy sharing process. Node 3 shares 35% of its energy with node 2, which receives 28% due to 20% loss rate. Then, node 2 keeps 8% for itself and shares the remaining 20% with node 1, which receives only 16% and reaches 23%.

While multi-hop based energy sharing can help reach a perfect energy balance when single hop exchanges cannot, there are some additional challenges that need to be addressed. That is, the average time required until an energy balance occurs as well as the loss during energy exchanges can increase as more hops result in more loss. Thus, for the efficient modeling of this problem, we will allow the linear program to only use paths that are viable within the time constraint and has the least number of hops. To this end, we find the paths from all possible source nodes to all possible destinations and discard the paths that cannot provide an energy transfer with a probability p over the nodes on that path by the time threshold. Then, we find the shortest hop path among the paths selected for each pair and use this path in the linear program to compute energy exchanges and energy loss. If there are multiple same hop paths, then we select the path that can achieve the energy transfer with the highest probability among them.

5.1. Optimal energy balance

Let G denote the (undirected connected) contact graph of nodes in the network and let $p^h_{u,u'} = \langle u_1, u_2, u_3, \ldots, u_h \rangle$ be a path of h hops from node u to node u' in G where $u_1 = u$ and $u_h = u'$. As we assume that the intermeeting times of nodes i and j are defined with an independent random variable $X_{ij} \sim Exp(\lambda_{ij})$, the energy transfer time from node u to node u' on $p^h_{u,u'}$ can be modeled with a random variable $X^h_{u,u'} = \sum_{i=1}^{h-1} X_{u_i,u_{i+1}}$. Here, with a common $\lambda = \lambda_{u_i u_j}$, $\forall u_i \neq u_j \in [1, h]$,

this will convert to gamma distribution [56], $\Gamma(h,\lambda)$, and for different rates, one can calculate the actual CDF of $X^h_{u,u'}$, or $F_{X^h_{u,u'}}$, where the mean will be equal to $E[X]=\sum_{i=1}^{h-1}\frac{1}{\lambda_{u_i,u_{i+1}}}$ [57].

Let $\vec{\mathcal{P}}_u$ denote the set of all possible $p^h_{u,u'}$s in graph G from a source node u to any node u' for all h such that $F_{X^h_{u,u'}}(\tau)\geq p$, where p is the predefined minimum expected meeting probability as used in Section 4. Consider a new subgraph $G'_u\subset G$ such that all the edges in this new graph corresponds to the edges, $\vec{e}_{u,u'}\in\vec{\mathcal{P}}_u$. In order to reduce the loss during multi-hop based energy sharing and balancing process, we need to use the path with the minimum hop that can achieve an energy exchange within the time threshold. Thus, we set a weight of 1 for each edge in G'_u and apply Dijkstra's shortest path algorithm to identify the minimum hop path from source u to each destination in G'_u. Let $\boldsymbol{L}$ be an $m\times m$ matrix, where $\boldsymbol{L}_{u,u'}$ shows the minimum hop distance from node u to node u' in G'_u (we set $\boldsymbol{L}_{u,u'}=\infty$ if there is no such path). Since single hop based energy balancing, if possible, should be preferred over multi-hop based balancing as it will have lower loss, we set the objective function such that it also prioritizes using single hop over multi-hop after the priorities defined in single hop objective function. Let h_s be the total number of single hop energy exchanges used, which can be given as:

$$h_s=|\{(u,u')\mid u,u'\in\mathcal{M},u'\neq u,\epsilon_{u,u'}>0,\ L_{u,u'}=1\}|$$

Similarly, let h_m be the total number of multi-hop energy exchanges used, which can be given as:

$$h_m=|\{(u,u')\mid u,u'\in\mathcal{M},u'\neq u,\epsilon_{u,u'}>0,\ L_{u,u'}>1\}|$$

Total energy loss in the network can also be computed as:

$$\mathcal{L}=\sum_{\forall u}\sum_{\forall u'\neq u}(\epsilon_{u,u'}\times(1-(1-\beta)^{L_{u,u'}}))$$

The optimization model used in single hop case can then be extended to multi-hop energy balancing problem as:

$$\min\ (\mathcal{M}^2\times(\mathcal{M}^2\times(\delta(\mathcal{E}_f,\mathcal{V}_f)m+\mathcal{L})+h_s)+h_m) \tag{11}$$

$$\text{s.t.}\ \ 0\leq\epsilon_{u,u'}\leq E_t(u)l_{uu'}\qquad\forall(u,u') \tag{12}$$

$$0\leq\sum_{\forall u'\neq u}\epsilon_{u,u'}\leq E_t(u)\qquad\forall u \tag{13}$$

$$k_{uu'}+k_{u'u}\leq 1\qquad\forall(u,u') \tag{14}$$

$$\text{where}\ \ \epsilon_{u,u'}\ \text{is a decimal in}\ [0,1]\qquad\forall(u,u') \tag{15}$$

$$k_{uu'}=\begin{cases}1, & \text{if } \epsilon_{u,u'}>0\\ 0, & \text{otherwise}\end{cases}\qquad\forall(u,u') \tag{16}$$

$$l_{uu'}=\begin{cases}1, & \text{if } L_{u,u'}\neq\infty\\ 0, & \text{otherwise}\end{cases}\qquad\forall(u,u') \tag{17}$$

In the objective function (11), in order to make sure that single hop paths are prioritized over multi-hop paths we again use scalarization method. That is, we first multiply the single hop energy balancing objective by a constant ($\mathcal{M}^2$) and add the number of single hop energy exchanges. We then multiply the overall term by the same constant and add multi-hop counts. Note that each constant is selected as it is described in single hop case such that the previous prioritized objective will be preferred over the next one. Similarly, we update the constraints for energy exchange bounds in (12) where $l_{uu'}$ now specifies if there is a path from node u to node u' in G'_u, i.e., $l_{uu'}$ is set to 1 if $L_{u,u'}$ is equal to some finite number of hops. Otherwise, $l_{u,u'}$ is set to 0 if there is no path from node u to node u' in G'_u (i.e., $L_{u,u'}=\infty$). With $l_{u,u'}=0$, we again do not allow any energy exchange between nodes. Note that (13) still limits the total energy shared by a node (to any single and multi-hop node) by its own energy and allows the relay nodes preserve their own energy when relaying energy from other sources.

5.2. Energy balancing protocol

Similar to the single hop case, we adopt a *linear exact* energy balancing protocol which lets the meeting nodes exchange energy that is given by the linear program. However, using linear exact for multi-hop based energy balancing is not straightforward as it is for single hop. This is because a node acting as a relay might need to relay more energy than it can hold. Also, in order to avoid the temporary out-of-energy situations for nodes, we do not allow the relay nodes to transfer energy upon opportunistic contact with next hop nodes unless they have received energy from previous hop nodes.[2] This requires nodes to maintain information on energy amount to be transferred from its own energy as well as energy amount that is received from other sources and will be forwarded as a relay.

Let $\epsilon_{u,u'}$ be the energy amount that needs to be transferred from node u to node u', over single hop or multiple hops, to achieve the optimal solution found by the multi-hop MILP. Also, let $\epsilon^s_{u,u'}$ be the amount of u's self energy that needs to be shared to u' (for u' and all other nodes using u' as relay). Note that this also refers to the energy amount that node u can transfer to node u' without waiting for any energy reception from other nodes. Similarly, let $\epsilon^o_{u,u'}$ denote the amount of energy to be transferred from node u to u' where node u is acting as a relay for energy from other sources. In order to compute the values of $\epsilon^s_{u,u'}$ and $\epsilon^o_{u,u'}$, we also need to know the path used for energy exchanges by the linear program. In the subgraph G'_u, after applying Dijkstra's algorithm with edge weights set to 1, we can end up with multiple paths from node u to any other node u' with the same number of hops (h). In such cases, we select the path with the minimum expected time in order to increase the chance of completing the energy sharing within the time threshold. Let $p^{min}_{u,u'}$ be the minimum cost path from u to u' in G'_u, and let $\langle i,j\rangle$ denote the edge between nodes i and j. Then,

$$\epsilon^s_{u,u'}=\epsilon_{u,u'}+\sum_{k\in\mathcal{M},k\neq u,u'}(\epsilon_{u,k}\mid\langle u,u'\rangle\in p^{min}_{u,k})$$

$$\epsilon^o_{u,u'}=\sum_{\substack{k\in\mathcal{M},k\neq u,u'\\ d\in\mathcal{M},d\neq u,u',k}}(\epsilon_{k,d}\times(1-\beta)^{L_{k,u}}\mid\langle u,u'\rangle\in p^{min}_{k,d})$$

In the above equations, $\epsilon^s_{u,u'}$ is computed as the sum of energy to be transferred from u to u' and the total amount of energy to be transferred from u to every other destination in which u' is the first hop in its path. Similarly, $\epsilon^o_{u,u'}$ is calculated as the sum of total amount of energy to be transferred from all sources to all destinations in which u' is the next hop after u in its path. Note that we only take into account the energy amount that will reach node u after losses during transfers in previous hops (from the source node k to node u). After computation of necessary parameters, we can run this protocol as given in Algorithm 2.

In Algorithm 2, we divide the energy exchanges into two parts. In the first part (lines 1–9), we perform the energy exchanges originated from a node's self energy. In the second part (lines 10–19), we perform the energy exchanges due to a node's being relay between other nodes. Priority is given to the former. In the first part, we first calculate the amount of available energy that can be shared (line 4), and depending on the available space in the receiver, we determine the actual energy transfer that will happen (lines 5–6) and update the corresponding parameters based on the transferred amount. In the second part, we again first calculate the amount of available energy that can be shared (line 13), however this time we also consider the received energy as relay so far and only let such energy transfers after receiving sufficient energy from previous hops. Then, depending on the available space in the receiver, we again determine the actual energy transfer that will happen (lines 14–15) and update the parameters once it is performed (lines 16–19). Note that, different from the first part, as both the receiver and transmitter nodes are relays in the second part, the received energy amounts as relays are updated for both.

[2] Due to this restriction, we also do not develop equivalent of $\mathcal{P}_{OC}$ for multi-hop case.

Algorithm 2: P_{MLE}(u, u', $\epsilon^s_{u,u'}$, $\epsilon^o_{u,u'}$, r_u, t)

Input: (u, u'): Interacting nodes, t: Time of interaction
$\epsilon^s_{u,u'}$: Energy to be sent from u to u' directly
$\epsilon^o_{u,u'}$: Energy to be sent from u to u' as a relay
r_u: Received energy in node u as relay

for $\epsilon_{i,j} \in \{\epsilon^s_{u,u'}, \epsilon^s_{u',u}\}$ **do**
  if $(\epsilon_{i,j} > 0)$ **then**
    $(u^+, u^-) \leftarrow (i, j)$
    $\epsilon \leftarrow \min(E_{t-1}(u^+), \epsilon^s_{u^+,u^-})$
    if $(E_{t-1}(u^-) + \epsilon(1-\beta) > 100)$ **then**
      $\epsilon = 100 - \frac{E_{t-1}(u^-)}{(1-\beta)}$
    $(E_{t-1}(u^-), E_{t-1}(u^+)) = (E_{t-1}(u^-) + (1-\beta)\epsilon,\ E_{t-1}(u^+) - \epsilon)$
    $\epsilon^s_{u^+,u^-} = \epsilon^s_{u^+,u^-} - \epsilon$
    $r_{u^-} \leftarrow r_{u^-} + (1\text{-}\beta)\epsilon$
for $\epsilon_{i,j} \in \{\epsilon^o_{u,u'}, \epsilon^o_{u',u}\}$ **do**
  if $(\epsilon_{i,j} > 0)$ **then**
    $(u^+, u^-) \leftarrow (i, j)$
    $\epsilon \leftarrow \min(E_{t-1}(u^+), r_{u^+}, \epsilon^o_{u+,u-})$
    if $(E_{t-1}(u^-) + \epsilon(1-\beta) > 100)$ **then**
      $\epsilon = 100 - \frac{E_{t-1}(u^-)}{(1-\beta)}$
    $(E_{t-1}(u^-), E_{t-1}(u^+)) = (E_{t-1}(u^-) + (1-\beta)\epsilon,\ E_{t-1}(u^+) - \epsilon)$
    $\epsilon^o_{u^+,u^-} = \epsilon^o_{u^+,u^-} - \epsilon$
    $r_{u^+} \leftarrow r_{u^+} - \epsilon$
    $r_{u^-} \leftarrow r_{u^-} + (1\text{-}\beta)\ \epsilon$

6. Simulations

In this section, we evaluate the performance of the proposed energy balancing protocols through simulations. Next, we first list the protocols compared with brief descriptions, provide the performance metrics used, and describe the details of the simulation settings. Then, we provide the simulation results and discuss the impact of several parameters on results.

6.1. Energy balancing protocols in comparison

Below are the brief descriptions of all protocols compared through simulations:

- $\mathcal{P}^*_{OA}$: This *O*nline *A*verage protocol is the updated version of the state-of-the-art protocol $\mathcal{P}_{OA}$ proposed in [24–26]. The protocol simply lets the nodes in opposite sides of the current average energy in the network interact and split their energies equally. In the original $\mathcal{P}_{OA}$, each node locally estimates the average energy level in the network using the ratio of the total energy of the encountered nodes to the number of encountered nodes, which may not be accurate. As we allow computation of MILP results at a node or a server by knowing the energy levels of all nodes, for a fair comparison we assume the same for $\mathcal{P}_{OA}$ and name it as $\mathcal{P}^*_{OA}$, which performs better than $\mathcal{P}_{OA}$. Moreover, we use E_{opt} obtained from MILP results to decide the boundary between opposite sides in $\mathcal{P}^*_{OA}$, which helps decreasing energy loss.
- $\mathcal{P}_{LE}$: In the *L*inear *E*xact protocol, when the nodes meet, they only share the exact amount of energy that MILP solution with only single hop energy exchanges (obtained[3] by IBM CPLEX solver [58]) finds to reach the E_{opt} with minimum possible variation and loss after that, as described in Algorithm 1.
- $\mathcal{P}_{OC}$: In the *O*pportunistic *C*loser protocol, E_{opt} is obtained via MILP (with single hop energy exchanges) as in $\mathcal{P}_{LE}$, but the nodes opportunistically try to reach E_{opt}. That is, they do not wait for the other nodes that they are supposed to exchange energy with, as found by MILP, but utilize every meeting opportunity with the nodes in the opposite side. The one with closer energy level to E_{opt} is given priority to reach it first as described in Algorithm 1.
- $\mathcal{P}_{MLE}$: In the *M*ulti-hop *L*inear *E*xact protocol, we first find the E_{opt} by MILP solution using multi-hop energy exchanges (obtained by IBM CPLEX solver [58]) and then depending on the actual self and relayed energy amounts calculated, we let the meeting nodes share the exact amount of energy they are supposed to exchange, as described in Algorithm 2.

Note that there is no opportunistic version of $\mathcal{P}_{MLE}$ algorithm, as nodes in more than one hop distance away in the contact graph do not meet opportunistically.

6.2. Performance metrics

We use the following metrics in the performance comparison of the aforementioned protocols:

- *Total variation distance:* This is calculated by $\delta(\mathcal{E}_t, \mathcal{U}_t)$. That is, we find the ratio of the energy levels of nodes to the total energy in the network at each time, take the absolute difference from uniform distribution at that time and sum it for all nodes.
- *Total energy in the network:* This is the sum of energies at all nodes. As the nodes interact and exchange energy, due to the imperfect transfer efficiency the total available energy in the network decreases.
- *Number of interactions:* This is the number of interactions between nodes during which an energy exchange happens towards reaching a balance. It shows how selective the protocol is and hence it affects the efficiency of the protocol.
- *Total variation distance at a given total energy:* As the performance of the protocols may vary based on total variation distance and total energy in the network, we use this combined metric as an indicator of true performance.
- *Total variation distance at a given number of interactions:* Similarly, we use this metric to understand the impact of necessary interactions towards reaching the minimum possible total variation distance.

Note that as each protocol depends on E_{opt} calculated from MILP model at a central server, the initial computation and communication cost for all protocols will be the same. The additional computation and communication costs will come from the node interactions they result in. Thus, the performance results showing the number of interactions can also be used to compare their computation and communication cost differences.

6.3. Contact traces

We use both real and synthetic user traces to define the meeting relations between the nodes in the network. Real traces are obtained from one of the commonly used datasets in DTN literature [59] that is used for performance analysis of routing algorithms. With synthetic traces, we aim to generate different contact graphs with various sparsity levels.

- **Cambridge traces:** These are the Bluetooth recordings between the iMotes carried by 36 students from Cambridge University for a duration of almost two months. While Bluetooth has a range in the order of several meters, we use these interactions as an indication of nodes in close proximity of each other and assume that they can communicate and agree to come closer to perform energy exchange operation if needed.

[3] We set the MILP gap tolerance to 0 to make sure the results obtained are optimal.

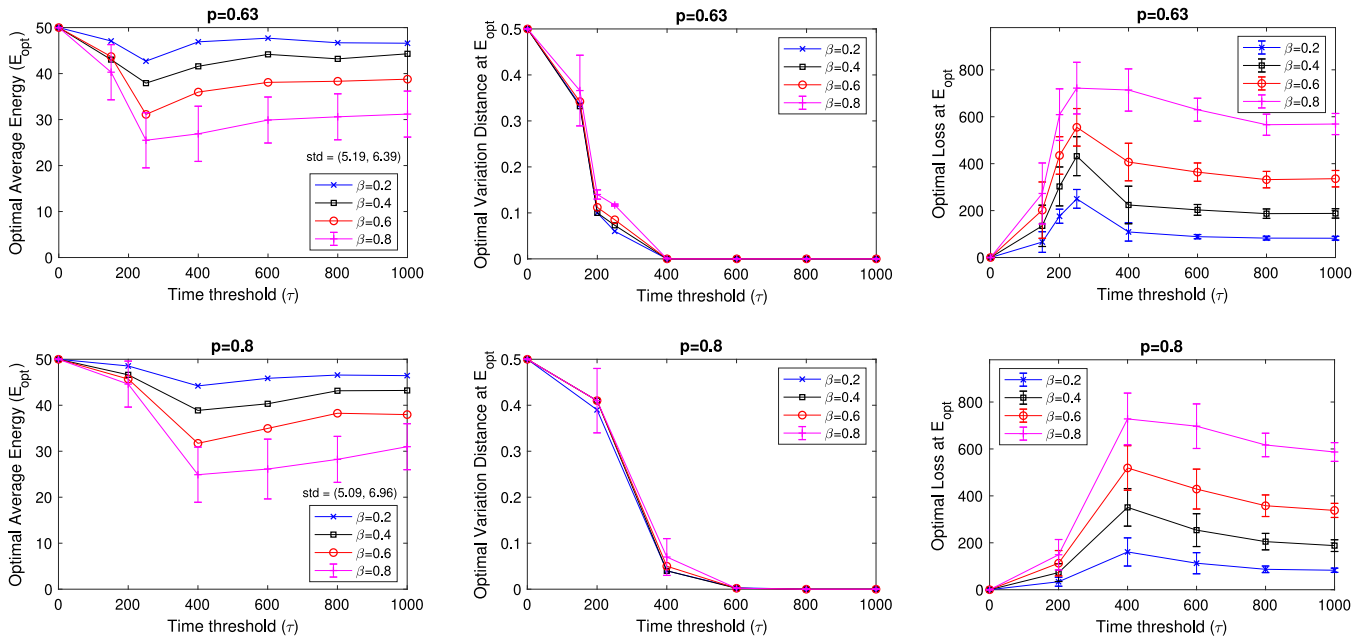

Fig. 3. Impact of time threshold (τ) and loss rate (β) on optimal average energy achievable (E_{opt}) and corresponding variation distance and total loss at E_{opt} with expected meeting probability threshold $p = 1 - 1/e = 0.63$ and $p = 0.8$ (For visual clarity, error bars are only shown for one line in top four figures as they are similar in others).

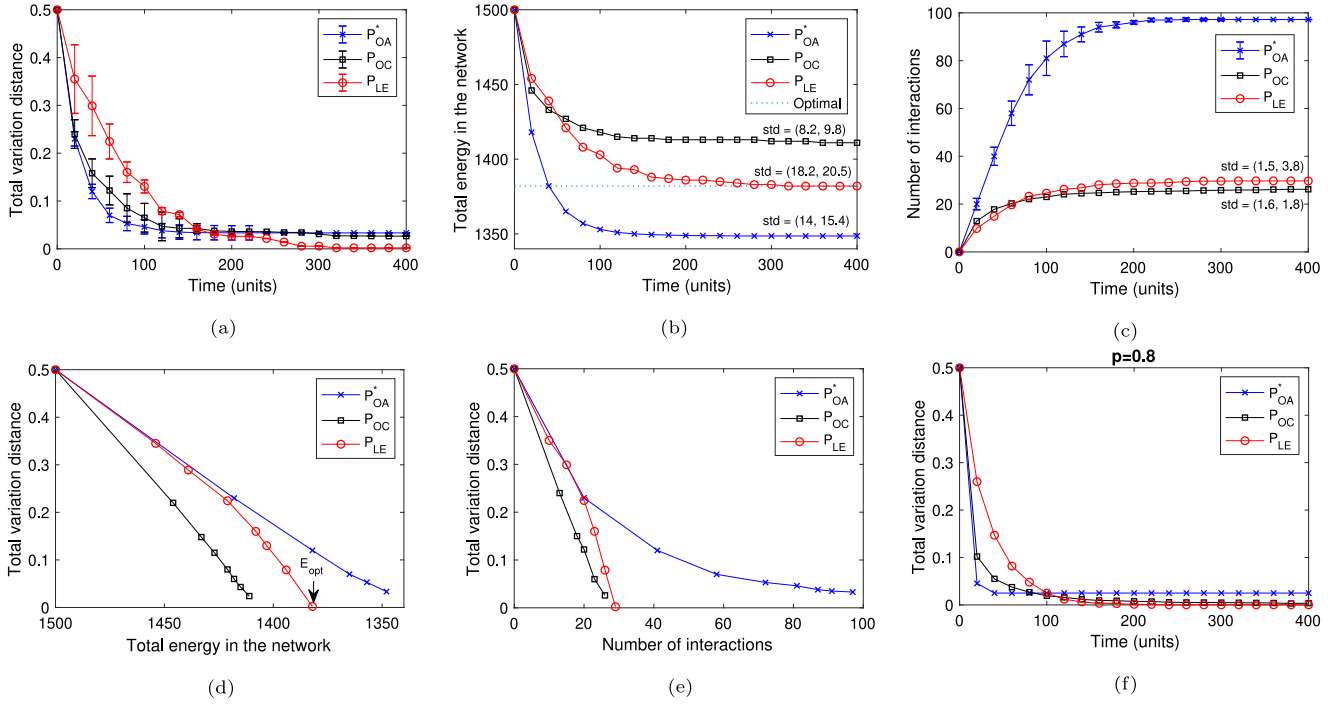

Fig. 4. Comparison of protocols in terms of (a) variation distance, (b) total energy remaining in the network, (c) total number of interactions, (d) variation distance at each total energy level and (e) variation distance at each total number of interactions (when $\beta = 0.2$, $\tau = 400$ time units, $p = 0.63$) using regular synthetic traces. (f) shows variation distance with p = 0.8 (For visual clarity, standard deviations (std) are shown in text if presenting them via error bars causes overlaps).

- **Regular synthetic traces:** These traces are generated for 30 nodes that meet with an exponentially distributed intermeeting time with a mean selected randomly between [100, 1500] time units. Through simulations, different time thresholds are also used to generate contact graphs with different average neighbor counts.
- **Group-based synthetic traces:** In order to show the benefits of multi-hop based energy exchanges during energy balancing process in particular, we use 30 nodes divided into two equal groups and allow nodes within each group meet up to 40% of other nodes in their own group and meet with a node in the other group with probability γ, which is set to 3% by default. However, we look at the impact of different γ on results. Intermeeting times are generated with an exponential distribution with a mean selected randomly between [100, 300] time units. We selected a smaller upper bound to allow multi-hop paths within time threshold.

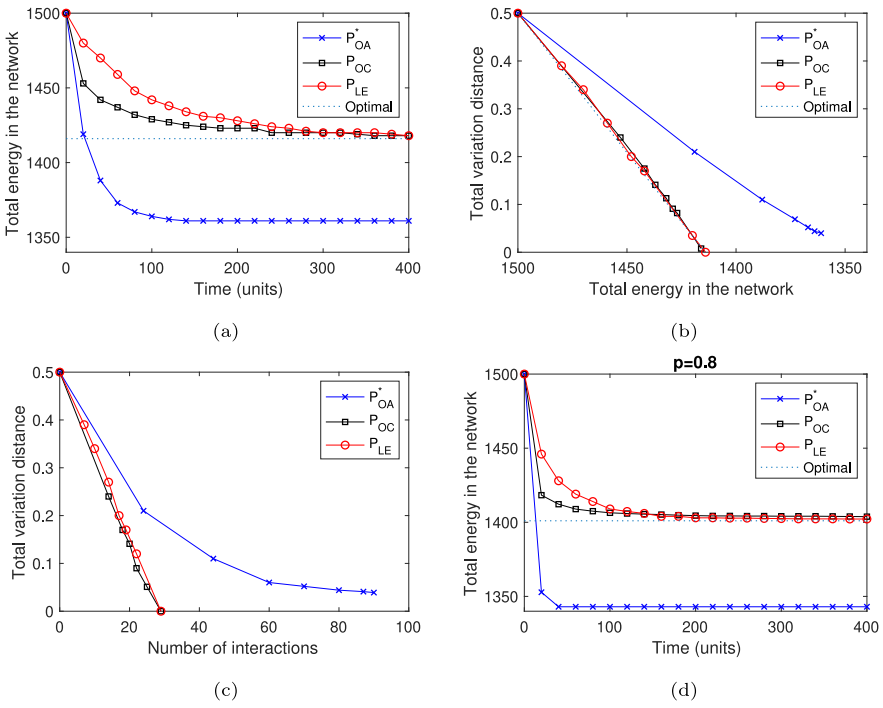

Fig. 5. Comparison of protocols in terms of (a) total energy remaining in the network, (b) variation distance at each total energy level and (c) variation distance at each total number of interactions (when $\beta = 0.2$, $\tau = 1000$ time units, $p = 0.63$) using regular synthetic traces. (d) shows total energy remaining in the network with p = 0.8.

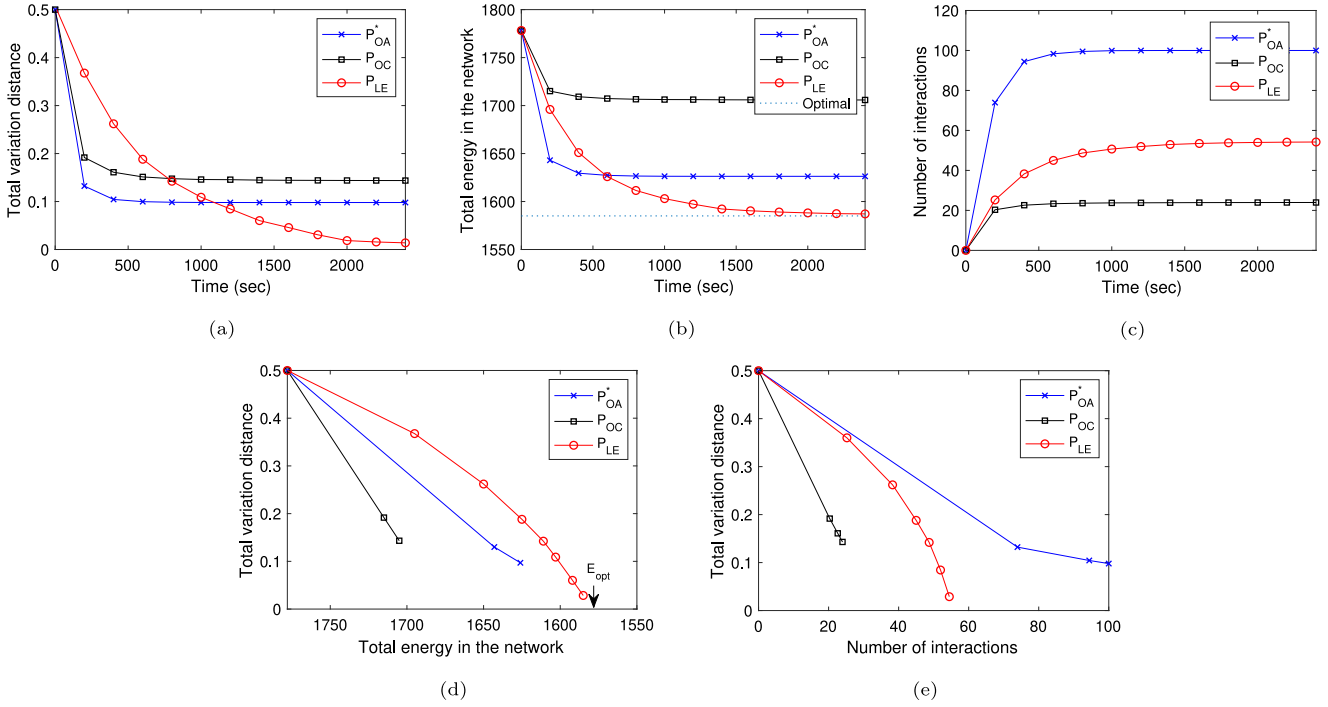

Fig. 6. Comparison of protocols in terms of (a) variation distance, (b) total energy remaining in the network, (c) total number of interactions, (d) variation distance at each total energy level and (e) variation distance at each total number of interactions (when $\beta = 0.2$, $\tau = 5000$ s, $p = 0.63$) using Cambridge traces.

Note that depending on the energy sharing technology used between nodes, the proximity requirements and corresponding energy transfer efficiency might be different. While we assume a default energy loss rate, $\beta = 0.2$ (i.e., 80% transfer efficiency) for main simulations, we look at the impact of this parameter in our results. Moreover, we assume that when nodes meet, they stay close enough to each other until they can achieve the required energy transfer under the energy balancing protocol in use, as in previous work [18,24–27]. The results with different transfer efficiency however can be considered as the relaxation of this assumption to some extent.

6.4. Simulation results

In this section, we present the results of our evaluation through simulations.[4] From the beginning of the simulation, we let the devices interact following their exponentially distributed intermeeting times and exchange energy based on the characteristics of each energy balancing protocol compared. Each simulation is repeated 100 times for statistical smoothness. The energy levels of nodes are uniformly distributed in (0–100]% in general. However, for the group-based synthetic contact traces generated for multi-hop protocol evaluation, we consider one group with nodes having high energy (i.e., $\geq 50\%$) and the other group with nodes having less energy (i.e., $< 50\%$). Moreover, we use two values for expected meeting probability p within time threshold, namely, $1-1/e \sim 0.63$ and 0.8. Note that, for example in the single hop case, the former simply considers the edges in the contact graph with average intermeeting time less than or equal to τ, and the latter requires the edges to have an average intermeeting time less than or equal to $\approx \tau/1.6$.

6.4.1. Results with regular synthetic traces

In Fig. 3, we first show the optimal energy balance (E_{opt}) achievable in contact graphs with different sparsity. To this end, we use regular synthetic traces and for different time thresholds (τ) and loss rates (β) we calculate the optimal average energy reachable with single hop exchanges[5] and corresponding variation distance and total loss at E_{opt} for two different p values. Note that as τ decreases the contact graph gets sparser as the edges between some pairs cannot achieve the expected meeting probability p by τ anymore, thus are removed from the graph. As the results show, optimal variation distance gets lower as τ increases and hits zero around $\tau = 400$ time units when $p = 0.63$. The loss associated with this optimal variation distance on the other hand increases initially and gets smaller later. This is because with smaller τ values, some nodes either have very small contacts or are totally isolated from others. Thus, perfect energy balance with zero variation distance was not possible. However, once this threshold is exceeded, the loss could be lowered by finding better energy exchange schedules. Note that E_{opt} results are also inline with this reasoning. Moreover, we see that as β increases, the optimal average energy achievable with different time thresholds decreases but it follows a similar pattern at different loss rates. Similarly, with $p = 0.8$, we obtain an expanded but similar pattern in all graphs compared to $p = 0.63$. This is because a time threshold $\tau = \tau_1$ with $p = 0.63$ will yield the same contact graph with a time threshold $\tau = 8\tau_1/5$ with $p = 0.8$.

In Fig. 4, we compare all protocols[6] in terms of aforementioned performance metrics using regular synthetic traces. In Fig. 4a, we see that P_{LE} can achieve the lowest variation distance among others. P^*_{OA} and P_{OC} have a similar variation distance which is slightly higher than the variation distance of P_{LE}. However, when we look at the total energy levels in the network shown in Fig. 4b, we observe that P^*_{OA} sacrifices a lot of energy during the energy balancing process. On the other hand, P_{OC} keeps more energy in the network even more than P_{LE}. This is because as it uses some unscheduled energy exchange opportunities towards the optimal average energy level, it diverges from optimal variation distance but this does not cause losing energy in the network unnecessarily. Moreover, the number of interactions between nodes in P^*_{OA} is the highest among all compared protocols, as shown in Fig. 4c, while proposed protocols limit the interactions. When we compare the variation distance at the same total energy in the network in Fig. 4d, we observe that P^*_{OA} indeed has the worst performance. On the other hand, P_{LE} reaches the optimal energy level and decreases the total variation distance gradually. Here, P_{OC} shows an interesting behavior as it achieves a better variation distance at a given total energy in the network but it cannot reach the smallest possible variation distance as P_{LE} does. Thus, if some variation distance is tolerable, P_{OC} can be considered performing better than P_{LE}. Moreover, P_{OC} achieves this with smaller variation distance at a given interaction count than other protocols, as it is shown in Fig. 4e. P^*_{OA} again performs the worst due to its design. In order to show the impact of p, we provide the variation distance results as a representative in Fig. Fig. 4f. As expected, all protocols achieve a smaller variation distance in earlier times. One interesting observation here is, P_{OC} can achieve zero variation distance which was not possible when $p = 0.63$. This is because larger p allows energy exchanges only between nodes that are more likely to meet. Note that, while using larger p is desirable, it can cause the contact graph be partitioned and make the zero variation distance impossible. We discuss the situation in disconnected graphs in the next section.

In the results shown in Fig. 5, we relax the time threshold and set it to $\tau = 1000$ time units in order to increase the contact graph density and the energy exchange opportunities. Here, only results with three metrics are shown for the sake of brevity. We observe that with this increased time threshold, the total energy kept in the network increases (i.e., loss decreases). P_{OC} also causes more loss initially which is not the case in earlier results. Another significant change is that the performances of P_{OC} and P_{LE} get closer in terms of total variation distance at a given total energy and number of interactions. These can be explained by the increased energy exchange opportunities. With $p = 0.8$, as shown in Fig. 5d, total energy in the network decreases quickly due to earlier happening link selections, but eventually this also causes slightly more energy loss due to the decreased energy exchange opportunities.

6.4.2. Results with cambridge traces

Next, we compare the performance of all protocols using Cambridge traces. In Fig. 6a, we see that P_{LE} provides close to zero variation distance and performs the best compared to others. Interestingly, P^*_{OA} achieves better variation distance than P_{OC}, which was not the case in regular synthetic traces. However, as it is shown in Fig. 6b, P^*_{OA} causes more loss in the network compared to P_{OC}. P_{LE} reaches the optimal energy in the network with the smallest possible variation distance. In terms of total variation distance at a given total energy level, P_{OC} performs better than others for earlier energy levels, but it cannot reach the variation distance others can do, as shown in Fig. 6d. The interactions for P^*_{OA} is the highest again among all protocols while P_{OC} has the smallest interactions that is also considerably less than the interactions of P_{LE} which was not the case in regular synthetic traces. This is because in Cambridge traces, the contact graph density is smaller than it is in regular synthetic traces and P_{OC} stops interacting further when nodes greedily reach the target.

6.4.3. Results with group-based synthetic traces

In Fig. 7, we show the results with group-based synthetic traces which are particularly generated in order to show the benefit of P_{MLE} over P_{LE} clearly. From Fig. 7, we observe that P_{MLE} achieves the smallest variation distance and keeps more energy in the network, while it increases the number of interactions slightly. This is because, as the hop distance between high energy nodes and low energy nodes increases, which is the case in these group-based synthetic traces, protocols considering only single hop based energy exchanges will offer limited energy transfer opportunities. Note that a node cannot share more than what it has in both single hop and multi-hop cases. However, multi-hop case allows energy transfers between nodes that are more than one hop away in contact graph through the help of intermediate nodes. Thus, a node with more energy can transfer its excessive energy to a node with low energy even it is multi-hop away. The multi-hop

[4] The simulations code is available at https://github.com/aashish33128/Energy-Balancing-Journal.

[5] We discuss the impact of using multi-hops on E_{opt} in Fig. 7.

[6] As the results for P_{MLE} are similar to P_{LE} results in regular synthetic and Cambridge traces, we do not show them in corresponding figures. We show P_{MLE} results explicitly only when group-based synthetic traces are used.

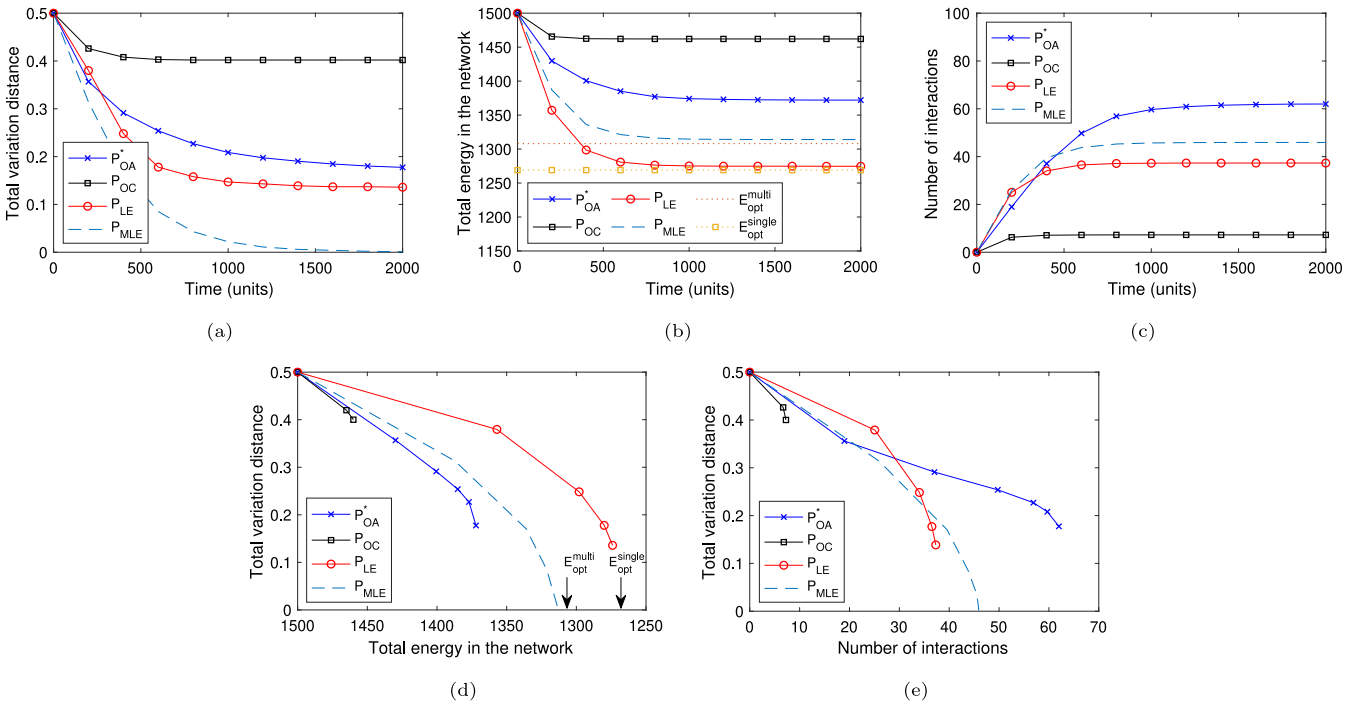

Fig. 7. Comparison of all algorithms in terms of (a) variation distance, (b) total energy remaining in the network, (c) total number of interactions, (d) variation distance at each total energy level and (e) variation distance at each total number of interactions (when $\beta = 0.2$, $\tau = 2000$, $p = 0.8$) using group-based synthetic traces.

energy transfers indeed eventually allow achieving a zero variation distance if the contact graph is connected. One interesting observation in Fig. 7b is that optimal energy balance (E_{opt}) in multi-hop case is more than it is in single hop case. This is because even though single hop exchanges may not allow reaching perfect energy balance, they leverage all possible single hop interactions and try to reduce the variation distance as much as possible. This then causes some unnecessary interactions and associated loss. Note that P_{OC} has the least amount of energy loss since the protocol cannot find useful interactions to reduce the variation distance. Moreover, P_{MLE} has more interactions than P_{LE} but it is still smaller than the number of interactions in P_{OA}.

In order to show the impact of inter-group sparsity γ on the benefit offered by multi-hop based energy exchanges, we obtain the results in Fig. 8 with different γ values in group-based synthetic traces. As the results show, with increasing γ, the performances of P_{MLE} and P_{LE} get closer. This is because larger γ connects more nodes between two groups thus decreases the hop distance between low energy nodes and high energy nodes. This makes zero optimal variation distance possible with single hop energy exchanges, thus even P_{MLE} starts using single hop interactions rather than multi-hop interactions to prevent unnecessary energy loss. Note that with $\gamma = 0$, the contact graph will be disconnected and no interactions will be helpful to reduce variation distance further as they will be all between same side nodes.

7. Discussion on network lifetime maximization

In this section, we discuss the relation between the energy balancing problem and network lifetime maximization problem. As it is also highlighted in previous studies [24–27], one of the goals of energy balancing process is to prolong the network lifetime. However, the relation of energy balancing and network lifetime has not been elaborated in these studies. Network lifetime is usually defined as the time until one of the nodes in the network dies due to energy depletion. Thus, network lifetime maximization problem can simply be defined as maximizing the minimum energy level of the nodes (assuming that energy consumption rates after energy exchanges completed are the same for each node) in the network through energy exchanges in opportunistic meetings. The objective for this problem can then be defined as:

$$\max(\min\{E_f(u)\ \forall u\}) \tag{18}$$

where $E_f(u)$ is the final energy level of node u. Here, as opposed to the objective function in energy balancing problem, the objective function in lifetime maximization problem is not concerned about the variation distance and the total loss in the network as the main priority is increasing the energy of the node with the minimum energy level. However, the constraints of energy balancing problem are still valid with lifetime maximization objective since the interactions of nodes still depend on the node relations and the amount of energy available.

If a perfect energy balance is possible in a network (i.e., zero variation distance) such that all nodes have the same energy level, the maximum network lifetime will also be achieved. That is, these two problems converge to each other. Moreover, we know that P_{MLE} will always achieve the perfect balance if the contact graph among nodes is connected. Thus, in such networks, energy balancing and network lifetime maximization result in the same outcome. However, if the contact graph is not connected (e.g., due to the removal of links due to time threshold τ), or the protocol cannot achieve the zero variation distance (e.g., P_{LE} may not achieve a perfect balance even if the contact graph is connected), the final energy distribution of nodes after energy balancing process may not result in the maximum network lifetime achievable. Thus, the objective should be updated as (18).

In order to show the difference in the outcomes of energy balancing and network lifetime maximization problems, we obtain results in group-based synthetic traces. Fig. 9 shows the network lifetime obtained with balancing and maximum lifetime objectives when $\gamma = 0.03$ and $\gamma = 0$ (i.e., network is disconnected). Comparing Fig. 9a and b, we observe that P_{MLE} can achieve the same network lifetime with both objective functions. This is because P_{MLE} can reach zero variation distance by $\tau = 2000$ as shown in Fig. 7a. On the other hand, we see that with maximum lifetime objective, network lifetime increases earlier than it does with balancing function. This is because the outcomes of the two objectives overlap only at the end (i.e., when perfect balance is obtained) and maximum lifetime objective always

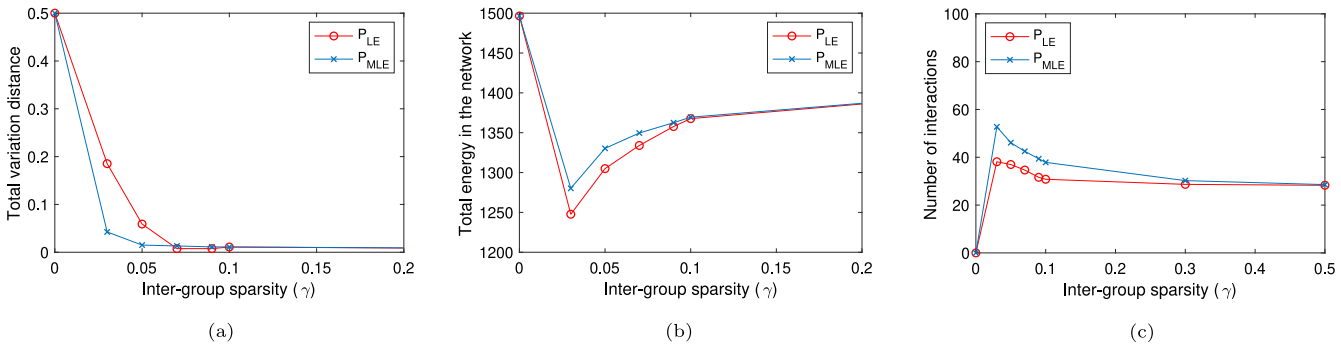

Fig. 8. Comparison of P_{LE} and P_{MLE} in terms of (a) variation distance, (b) total energy remaining in the network, and (c) total number of interactions under different inter-group contact sparsity (γ) in group-based synthetic traces ($p = 0.8$).

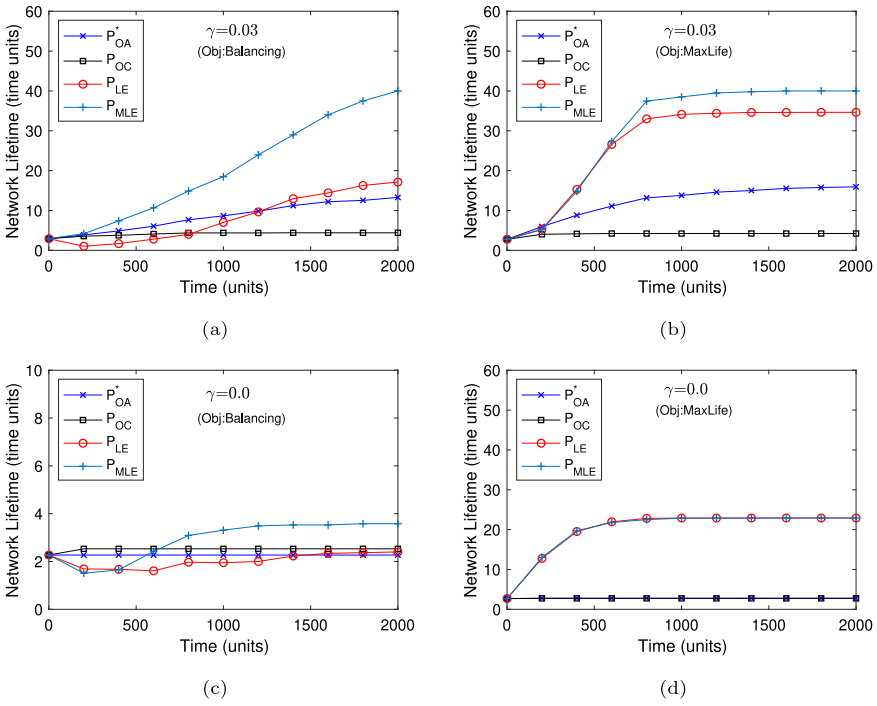

Fig. 9. Comparison of protocols in terms of achievable network lifetime with *balancing* and *lifetime maximization* objective functions and different γ values (when $\beta = 0.2$, $\tau = 2000$ time units, $p = 0.8$) using group-based synthetic traces.

considers network lifetime maximization target even before the time threshold is reached. Regarding the performance of P_{LE}, we see that it cannot achieve the same network lifetime with balancing objective as it obtains with maximum lifetime objective. This is because it cannot reach perfect balance by the time threshold thus both problems cannot converge to one another. P_{OC} and P^*_{OA} provide similar network lifetime with both objectives as the objective function change slightly affects their performance (i.e., average energy in the final network changes slightly so do the positive and negative node sets).

When $\gamma = 0$, the network is partitioned into two groups thus no energy transfer is possible between the nodes in different groups. Thus, the balancing (Fig. 9c) and lifetime maximization objectives (Fig. 9d) yield remarkably different energy exchanges among nodes towards their goals. The balancing objective tries to decrease the variation distance in the network as much as possible through energy exchanges between positive and negative side nodes which only exist in the low energy group. However, this yields a very small network lifetime for all protocols (with P_{MLE} offering slightly more lifetime than others). On the other hand, lifetime maximization objective can help P_{MLE} and P_{LE} achieve much higher lifetime with a focus on increasing the minimum energy level among the nodes in the low energy group. Note that as the nodes within each group have high contact density (i.e., 40%), P_{MLE} and P_{LE} perform similarly, however with a smaller intra-group contact density P_{MLE} will provide better lifetime than P_{LE} as in the case of Fig. 9b.

8. Conclusion

In this paper, we study the energy balancing problem among the nodes in a mobile opportunistic network. We aim to first balance the energy levels of nodes as much as possible and then minimize the energy loss during this process considering different relations among nodes as well as a time threshold to finish the balancing. To this end, we model the problem using Mixed Integer Linear Programming and propose different protocols based on its results. We initially consider

single hop based energy exchanges in our model. However, due to its limitations especially in sparse networks with long hop distances between low energy and high energy nodes, it cannot reach lower variation distances. Thus, we extend our model using multi-hop based energy exchanges, where nodes that are not meeting directly use relay nodes to exchange energy between them. We develop three different energy sharing protocols based on these models and through simulations using both synthetic and real user based traces we compare their performance with a state-of-the-art protocol. Results show that we can achieve better variation distance by keeping more energy in the network with the proposed protocols. Moreover, multi-hop based approach performs better than single hop based approach especially in sparse networks. Finally, through different network scenarios, we discuss on the implications of energy balancing process on network lifetime and propose modifications to the existing MILP model that aims to maximize the network lifetime directly instead of aiming to minimize variation distance and loss. With simulation results we show that especially in disconnected networks such modifications can help reach the maximum lifetime while energy balancing process cannot.

In our future work, we will study the energy balancing problem when the energy consumption due to the mobility and other activities of nodes are also considered in the balancing process. We will also look at several other issues such as load balancing and battery deterioration during the balancing process.

Declaration of competing interest

The authors declare that they have no known competing financial interests or personal relationships that could have appeared to influence the work reported in this paper.

Acknowledgment

This work was supported in part by NSF award CNS-1647217.

References

[1] H. Mostafaei, A. Montieri, V. Persico, A. Pescapè, A sleep scheduling approach based on learning automata for WSN partial coverage, J. Netw. Comput. Appl. 80 (2017) 67–78, http://dx.doi.org/10.1016/j.jnca.2016.12.022.

[2] T. Sanislav, S. Zeadally, G.D. Mois, S.C. Folea, Wireless energy harvesting: Empirical results and practical considerations for Internet of Things, J. Netw. Comput. Appl. 121 (2018) 149–158, http://dx.doi.org/10.1016/j.jnca.2018.08.002.

[3] J. Zuo, C. Dong, H.V. Nguyen, S.X. Ng, L.-L. Yang, L. Hanzo, Cross-layer aided energy-efficient opportunistic routing in ad hoc networks, IEEE Trans. Commun. 62 (2) (2014) 522–535.

[4] C. Lin, Y. Zhou, H. Dai, J. Deng, G. Wu, MPF: Prolonging network lifetime of wireless rechargeable sensor networks by mixing partial charge and full charge, in: 15th Annual IEEE International Conference on Sensing, Communication, and Networking, SECON, IEEE, 2018, pp. 1–9.

[5] S. Zhang, J. Wu, S. Lu, Collaborative mobile charging, IEEE Trans. Comput. 64 (3) (2015) 654–667, http://dx.doi.org/10.1109/TC.2013.2297926.

[6] C.-F. Cheng, C.-C. Wang, The energy replenishment problem in mobile WRSNs, in: 2018 IEEE 15th International Conference on Mobile Ad Hoc and Sensor Systems, MASS, IEEE, 2018, pp. 143–144.

[7] W. Xu, W. Liang, J. Peng, Y. Liu, Y. Wang, Maximizing charging satisfaction of smartphone users via wireless energy transfer, IEEE Trans. Mob. Comput. 16 (4) (2016) 990–1004.

[8] V. Iyer, E. Bayati, R. Nandakumar, A. Majumdar, S. Gollakota, Charging a smartphone across a room using lasers, ACM Interact. Mobile Wearable Ubiquitous Technol. 1 (4) (2018) 143.

[9] E. Bulut, S. Hernandez, A. Dhungana, B.K. Szymanski, Is crowdcharging possible? in: 27th International Conference on Computer Communication and Networks, ICCCN 2018, Hangzhou, China, July 30–August 2, 2018, 2018, pp. 1–9.

[10] D. Kosmanos, L.A. Maglaras, M. Mavrovouniotis, S. Moschoyiannis, A. Argyriou, A. Maglaras, H. Janicke, Route optimization of electric vehicles based on dynamic wireless charging, IEEE Access 6 (2018) 42551–42565.

[11] G. Buja, C.-T. Rim, C.C. Mi, Dynamic charging of electric vehicles by wireless power transfer, IEEE Trans. Ind. Electron. 63 (10) (2016) 6530–6532.

[12] R. Zhang, S. Zhang, Z. Qian, M. Xiao, J. Wu, J. Ge, S. Lu, Collaborative interactive wireless charging in a cyclic mobispace, in: IEEE/ACM International Symposium on Quality of Service, IEEE/ACM IWQoS 2018, 2018.

[13] X. Fan, H. Ding, S. Li, M. Sanzari, Y. Zhang, W. Trappe, Z. Han, R.E. Howard, Energy-Ball: Wireless power transfer for batteryless internet of things through distributed beamforming, ACM Interact. Mobile Wearable Ubiquitous Technol. 2 (2) (2018) 65.

[14] W. Fang, Q. Zhang, Q. Liu, J. Wu, P. Xia, Fair scheduling in resonant beam charging for IoT devices, IEEE Internet Things J. 6 (1) (2019) 641–653.

[15] A. Lakhdari, A. Bouguettaya, S. Mistry, A.G. Neiat, Composing energy services in a crowdsourced IoT environment, IEEE Trans. Serv. Comput. (2020).

[16] P. Worgan, J. Knibbe, M. Fraser, D. Martinez Plasencia, Powershake: Power transfer interactions for mobile devices, in: CHI Conference on Human Factors in Computing Systems, ACM, 2016, pp. 4734–4745.

[17] A. Dhungana, E. Bulut, Peer-to-peer energy sharing in mobile networks: Applications, challenges, and open problems, Ad Hoc Netw. 97 (2020) 102029.

[18] T.P. Raptis, When wireless crowd charging meets online social networks: A vision for socially motivated energy sharing, Online Soc. Netw. Media 16 (2020) 100069.

[19] A. Abusafia, A. Bouguettaya, S. Mistry, Incentive-based selection and composition of IoT energy services, 2020, arXiv preprint arXiv:2007.09985.

[20] Wireless Power Consortium, The Qi standard, 2020, URL https://www.wirelesspowerconsortium.com.

[21] Samsung, Micro USB battery power sharing cable, 2020, URL https://www.samsung.com/uk/mobile-accessories/power-sharing-cable-micro-5pin-sg900/.

[22] Q. Zhang, F. Li, Y. Wang, Mobile crowd wireless charging toward rechargeable sensors for Internet of Things, IEEE Internet Things J. 5 (6) (2018) 5337–5347.

[23] A. Dhungana, E. Bulut, Opportunistic wireless crowd charging of IoT devices from smartphones, in: 2020 16th International Conference on Distributed Computing in Sensor Systems, DCOSS, IEEE, 2020, pp. 1–6.

[24] S. Nikoletseas, T.P. Raptis, C. Raptopoulos, Energy balance with peer-to-peer wireless charging, in: IEEE 13th International Conference on Mobile Ad Hoc and Sensor Systems, MASS, 2016, pp. 101–108.

[25] S. Nikoletseas, T.P. Raptis, C. Raptopoulos, Wireless charging for weighted energy balance in populations of mobile peers, Ad Hoc Netw. 60 (2017) 1–10.

[26] S. Nikoletseas, T.P. Raptis, C. Raptopoulos, Interactive wireless charging for energy balance, in: 36th International Conference on Distributed Computing Systems, ICDCS, IEEE, 2016, pp. 262–270.

[27] A. Dhungana, E. Bulut, Loss-aware efficient energy balancing in mobile opportunistic networks, in: IEEE Global Telecommunications Conference, GLOBECOM, 2019, 2019, pp. 1–6.

[28] J. Dede, A. Förster, E. Hernández-Orallo, J. Herrera-Tapia, K. Kuladinithi, V. Kuppusamy, P. Manzoni, A. bin Muslim, A. Udugama, Z. Vatandas, Simulating opportunistic networks: Survey and future directions, IEEE Commun. Surv. Tutor. 20 (2) (2017) 1547–1573.

[29] D. Karamshuk, C. Boldrini, M. Conti, A. Passarella, Human mobility models for opportunistic networks, IEEE Commun. Mag. 49 (12) (2011) 157–165.

[30] A. Dhungana, E. Bulut, Mobile energy balancing in heterogeneous opportunistic networks, in: IEEE 16th International Conference on Mobile Adhoc and Sensor Systems, MASS, 2019, pp. 1–9.

[31] X. Hu, T.H. Chu, V.C. Leung, E.C.-H. Ngai, P. Kruchten, H.C. Chan, A survey on mobile social networks: Applications, platforms, system architectures, and future research directions, IEEE Commun. Surv. Tutor. 17 (3) (2014) 1557–1581.

[32] Y. Li, X. Zhu, D. Jin, D. Wu, Multiple content dissemination in roadside-unit-aided vehicular opportunistic networks, IEEE Trans. Veh. Technol. 63 (8) (2014) 3947–3956.

[33] V.F. Mota, F.D. Cunha, D.F. Macedo, J.M. Nogueira, A.A. Loureiro, Protocols, mobility models and tools in opportunistic networks: A survey, Comput. Commun. 48 (2014) 5–19.

[34] M. Conti, S. Giordano, M. May, A. Passarella, From opportunistic networks to opportunistic computing, IEEE Commun. Mag. 48 (9) (2010) 126–139.

[35] Y. Wu, Y. Zhao, M. Riguidel, G. Wang, P. Yi, Security and trust management in opportunistic networks: a survey, Secur. Commun. Netw. 8 (9) (2015) 1812–1827.

[36] S. Zakhary, A. Benslimane, On location-privacy in opportunistic mobile networks, a survey, J. Netw. Comput. Appl. 103 (2018) 157–170.

[37] X. Lu, P. Wang, D. Niyato, D.I. Kim, Z. Han, Wireless charging technologies: Fundamentals, standards, and network applications, IEEE Commun. Surv. Tutor. 18 (2) (2015) 1413–1452.

[38] L. Xie, Y. Shi, Y. Hou, A. Lou, Wireless power transfer and applications to sensor networks, IEEE Wirel. Commun. 20 (4) (2013) 140–145.

[39] D. Niyato, P. Wang, D.I. Kim, W. Saad, Finding the best friend in mobile social energy networks, in: IEEE International Conference on Communications, ICC, IEEE, 2015, pp. 3240–3245.

[40] E. Bulut, B.K. Szymanski, Mobile energy sharing through power buddies, in: Wireless Communications and Networking Conference, WCNC, IEEE, 2017, pp. 1–6.

[41] A. Dhungana, T. Arodz, E. Bulut, Exploiting peer-to-peer wireless energy sharing for mobile charging relief, Ad Hoc Netw. 91 (2019) 101882.

[42] Dhungana, Aashish and Arodz, Tomasz and Bulut, Eyuphan, Charging skip optimization with peer-to-peer wireless energy sharing in mobile networks, in: IEEE International Conference on Communications, ICC, 2018, pp. 1–6.

[43] E. Bulut, M.E. Ahsen, B.K. Szymanski, Opportunistic wireless charging for mobile social and sensor networks, in: Globecom Workshops, GC Wkshps, IEEE, 2014, pp. 207–212.
[44] D. Niyato, P. Wang, D.I. Kim, Z. Han, Content messenger selection and wireless energy transfer policy in mobile social networks, in: International Conference on Communications, ICC, IEEE, 2015, pp. 3831–3836.
[45] A. Dhungana, E. Bulut, Energy sharing based content delivery in mobile social networks, in: 20th International Symposium on "a World of Wireless, Mobile and Multimedia Networks", WoWMoM, IEEE, 2019, pp. 1–9.
[46] D. Niyato, P. Wang, D.I. Kim, W. Saad, Z. Han, Mobile energy sharing networks: Performance analysis and optimization, IEEE Trans. Veh. Technol. 65 (5) (2016) 3519–3535.
[47] A. Madhja, S. Nikoletseas, D. Tsolovos, A.A. Voudouris, Peer-to-peer energy-aware tree network formation, in: 16th International Symposium on Mobility Management and Wireless Access, ACM, 2018, pp. 1–8.
[48] A. Madhja, S. Nikoletseas, A.A. Voudouris, Energy-aware tree network formation among computationally weak nodes, Comput. Netw. 168 (2020) 107068.
[49] E. Wang, Y. Yang, J. Wu, Energy efficient beaconing control strategy based on time-continuous markov model in DTNs, IEEE Trans. Veh. Technol. 66 (8) (2017) 7411–7421.
[50] W. Gao, G. Cao, A. Iyengar, M. Srivatsa, Supporting cooperative caching in disruption tolerant networks, in: 2011 31st International Conference on Distributed Computing Systems, IEEE, 2011, pp. 151–161.
[51] C. Liu, J. Wu, An optimal probabilistic forwarding protocolin delay tolerant networks, in: 10th ACM International Symposium on Mobile Ad Hoc Networking and Computing, 2009, pp. 105–114.
[52] E. Bulut, Z. Wang, B.K. Szymanski, Cost-effective multiperiod spraying for routing in delay-tolerant networks, IEEE/ACM Trans. Netw. 18 (5) (2010) 1530–1543.
[53] C. Liu, J. Wu, On multicopy opportunistic forwarding protocols in nondeterministic delay tolerant networks, IEEE Trans. Parallel Distrib. Syst. 23 (6) (2012) 1121–1128.
[54] E. Bulut, B.K. Szymanski, Exploiting friendship relations for efficient routing in mobile social networks, IEEE Trans. Parallel Distrib. Syst. 23 (12) (2012) 2254–2265.
[55] E. Bulut, S.C. Geyik, B.K. Szymanski, Utilizing correlated node mobility for efficient DTN routing, Pervasive Mob. Comput. 13 (2014) 150–163.
[56] Gamma distribution, 2020, URL https://en.wikipedia.org/wiki/Relationships_among_probability_distributions.
[57] M. Bibinger, Notes on the sum and maximum of independent exponentially distributed random variables with different scale parameters, 2013, arXiv preprint arXiv:1307.3945.
[58] IBM CPlex Optimization Solver, 2019, URL https://www.ibm.com/products/ilog-cplex-optimization-studio.
[59] J. Leguay, A. Lindgren, J. Scott, T. Friedman, J. Crowcroft, Opportunistic content distribution in an urban setting, in: Proc. ACM SIGCOMM 2006 - Workshop on Challenged Networks, CHANTS, Pisa, Italy, 2006.

Aashish Dhungana received the BS degree from Kathmandu University in Nepal in 2014. He is now doing his Ph.D. in the Computer Science Department of Virginia Commonwealth University under the supervision of Dr. Eyuphan Bulut. His research interests include mobile social networks, Delay-tolerant networks, and Device-to-Device (D2D) communications and energy sharing. He is a member of IEEE.

Eyuphan Bulut received the Ph.D. degree in the Computer Science department of Rensselaer Polytechnic Institute (RPI), Troy, NY, in 2011. He then worked as a senior engineer in Mobile Internet Technology Group (MITG) group of Cisco Systems in Richardson, TX for 4.5 years. He is now an Associate Professor with the Department of Computer Science, Virginia Commonwealth University (VCU), Richmond, VA. His research interests include mobile and wireless computing, network security and privacy, mobile social networks and crowd-sensing. Dr. Bulut has been serving as an Associate Editor in IEEE Access. He is a senior member of IEEE and a member of ACM.